

Exploring the Limits of Historical Information for Temporal Knowledge Graph Extrapolation

Yi Xu, Junjie Ou, Hui Xu, Luoyi Fu, Lei Zhou, Xinbing Wang, *Senior Member, IEEE*, and Chenghu Zhou

Abstract—Temporal knowledge graphs, representing the dynamic relationships and interactions between entities over time, have been identified as a promising approach for event forecasting. However, a limitation of most temporal knowledge graph reasoning methods is their heavy reliance on the recurrence or periodicity of events, which brings challenges to inferring future events related to entities that lack historical interaction. In fact, the current state of affairs is often the result of a combination of historical information and underlying factors that are not directly observable. To this end, we investigate the limits of historical information for temporal knowledge graph extrapolation and propose a new event forecasting model called **Contrastive Event Network** (CENET) based on a novel training framework of historical contrastive learning. CENET learns both the historical and non-historical dependency to distinguish the most potential entities that best match the given query. Simultaneously, by launching contrastive learning, it trains representations of queries to probe whether the current moment is more dependent on historical or non-historical events. These representations further help train a binary classifier, whose output is a boolean mask, indicating the related entities in the search space. During the inference process, CENET employs a mask-based strategy to generate the final results. We evaluate our proposed model on five benchmark graphs. The results demonstrate that CENET significantly outperforms all existing methods in most metrics, achieving at least 8.3% relative improvement of Hits@1 over previous state-of-the-art baselines on event-based datasets.

Index Terms—Knowledge Graph, Contrastive Learning, Temporal Reasoning.

arXiv:2308.15002v1 [cs.AI] 29 Aug 2023

1 INTRODUCTION

KNOWLEDGE Graphs (KGs), serving as the structured representations of human knowledge, have revealed significant potential across a variety of domains, including natural language processing [2], [3], [4], recommendation systems [5], [6], and information retrieval [7], [8]. A conventional KG typically refers to a static knowledge base, which utilizes a graph-structured data topology to integrate facts (also known as events), represented as triples (s, p, o) , where s and o denote the subject and object entities respectively, and p represents the relation type, or predicate. In the real world, knowledge is constantly evolving, leading to the development of Temporal Knowledge Graphs (TKGs), where the fact has extended from a triple (s, p, o) to a quadruple with a timestamp t , i.e., (s, p, o, t) . As a result, a TKG consists of multiple snapshots, and the facts in the same snapshot co-occur. Figure 1 depicts an example of TKG consisting of a series of international political events, where some events may recur, and new events will also emerge.

TKGs provide new perspectives and insights for various downstream applications, e.g., policymaking [9], stock prediction [10], and dialogue systems [11], thus triggering

intense interests in TKG reasoning. In this work, we focus on forecasting events (facts) in the future on TKGs, also known as graph extrapolation. Our goal is to predict the missing entities of queries like $(s, p, ?, t)$ for a future timestamp t that has yet to be observed in the training set.

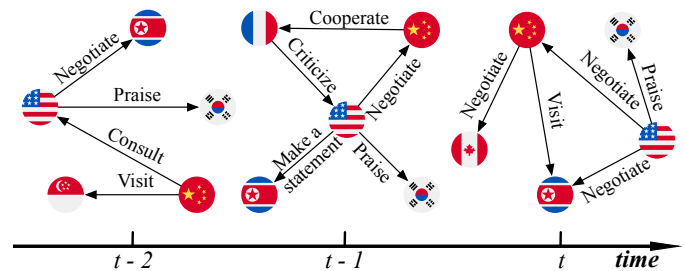


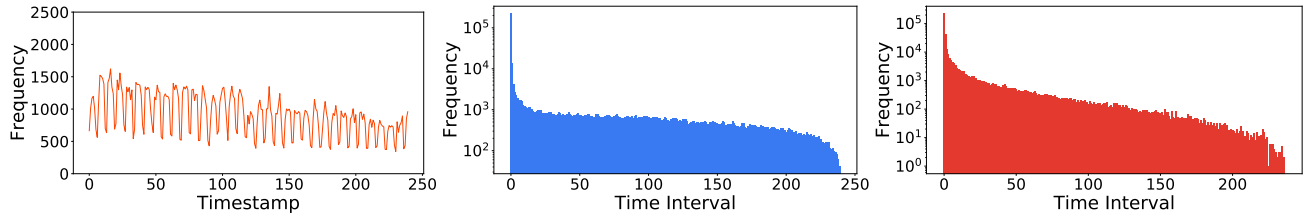
Fig. 1. An example of TKG with three snapshots.

Many efforts [12], [13] have been made toward modeling the structural and temporal characteristics of TKGs for future event prediction. Some mainstream examples [13], [14] make reference to known events in history, which can easily predict repetitive or periodic events. However, such methods share three major issues for graph extrapolation:

Challenge of predicting new events. In terms of the event-based TKG *Integrated Crisis Early Warning System*, new events that have never occurred before account for about 40% – 60% [15]. As seen from Figure 2 (a), new events continuously appear across all timestamps. It is challenging to infer these new events because they have fewer temporal interaction traces during the whole timeline. For instance, the right part of Figure 3 shows the query (*the United States, Negotiate, ?, t+1*) and its corresponding new events (*the United States, Negotiate, Russia, t+1*), where most existing

- This paper is an extended version of [1] which has been accepted for the presentation at the 37th AAAI Conference on Artificial Intelligence.
- Yi Xu, Hui Xu, and Luoyi Fu are with Department of Computer Science and Engineering, Shanghai Jiao Tong University, Shanghai 200240, China. Email: {yixu98, xhui_1, yiluofu}@sjtu.edu.cn.
- Junjie Ou and Xinbing Wang are with the Department of Electronic Engineering, Shanghai Jiao Tong University, Shanghai 200240, China. E-mail: {j_michael, xwang8}@sjtu.edu.cn.
- Lei Zhou is with the School of Oceanography, Shanghai Jiao Tong University, Shanghai 200240, China. E-mail: zhoule1588@sjtu.edu.cn.
- Chenghu Zhou is with the Institute of Geographical Science and Natural Resources Research, Chinese Academy of Sciences, Beijing 100101, China. E-mail: zhouch@lreis.ac.cn.

Luoyi Fu and Xinbing Wang are corresponding authors.



(a) Frequency of new events under different timestamps. (b) Frequency of time intervals between the first and current occurrence of repetitive events. (c) Frequency of time intervals between the latest and current occurrence of repetitive events.

Fig. 2. Statistics of new and repetitive events on ICEWS18 dataset.

methods often obtain incorrect results over such query due to their focus on the high frequent recurring events.

Information loss of repetitive events. Mainstream temporal knowledge graph models employ time-window [13], [14], [16], [17], [18], [19], [20], [21] to truncate historical sequences for the convenience of RNN modules. Nevertheless, it also leads to a significant loss of information when it comes to repetitive events. In Figure 2 (b) and (c), many events may recur in the short term, but their first occurrences can be traced back to over 200 timestamps ago. These models miss essential patterns and insights that a longer historical sequence could provide by only considering a limited period of time. Besides, the truncation of historical data can make it difficult for the model to detect periodicity or recurring patterns in the data. As a result, the model’s ability to accurately predict or infer future events is hindered.

Absence of bias in reasoning. During the inference process, existing methods rank the probability scores of overall candidate entities in the whole graph without any bias. We argue that bias is necessary when approaching the missing entities of different events. For repetitive or periodic events, models are expected to prioritize a few frequently occurring entities, and for new events, models should pay more attention to entities with less historical interaction.

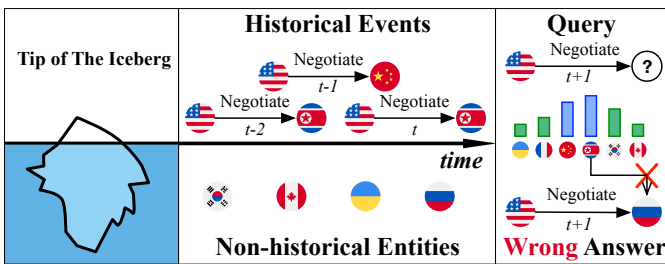


Fig. 3. Challenges of existing methods.

In this work, we will go beyond the limits of historical information and mine potential temporal patterns from the whole knowledge. To elaborate our design clearer, we call the past events associated with the entities in the current query $(s, p, ?, t)$ *historical events*, and others *non-historical events*. Their corresponding entities are called *historical* and *non-historical entities*, respectively. We will give formal definitions in Section 3.1. We intuitively consider that the events in TKG are not only related to their historical events but also indirectly related to unobserved underlying factors. The historical events we can see are only the tip of the iceberg.

We propose a novel TKG reasoning model called CENET (Contrastive Event Network) for event forecasting based on contrastive learning. Given a query $(s, p, ?, t)$ whose real object entity is o , CENET takes into account its historical and non-historical events and identifies significant entities via contrastive learning. Specifically, a copy mechanism-based scoring strategy is first adopted to model the dependency of historical and non-historical events, ensuring that there is no truncation operation on the entire timeline. In addition, all queries can be divided into two classes according to their real object entities: either the object entity o is a historical entity or a non-historical entity. Therefore, CENET naturally employs supervised contrastive learning to train representations of the two classes of queries, further helping train a classifier whose output is a boolean value to identify which kind of entities should receive more attention. During the inference, CENET combines the distribution from the historical and non-historical dependency, and further considers highly correlated entities with a mask-based strategy according to the classification results.

The contributions of our paper are summarized as follows:

- We examine the limits of historical information in existing TKG methods and propose a new model called CENET for event forecasting. CENET can predict not only repetitive and periodic events but also potential new events via joint investigation of both historical and non-historical information;
- To the best of our knowledge, CENET is the first model to apply contrastive learning to TKG reasoning, which trains contrastive representations of queries to identify highly correlated entities;
- We conduct experiments on five public benchmark graphs. The results demonstrate that CENET outperforms the state-of-the-art TKG models in the task of event forecasting.

The remainder of this article is organized as follows. Section 2 introduces the related work. Section 3 describes the details of our proposed model. The performance of CENET is verified in Section 4 with detailed analysis. Finally, Section 5 presents the conclusions and future work.

2 RELATED WORK

2.1 Temporal Knowledge Graph Reasoning

There are two different settings for TKG reasoning: interpolation and extrapolation [13], [22]. Given a TKG with times-

tamps ranging from t_0 to t_n , models with the interpolation setting aim to complete missing events that happened in the interval $[t_0, t_n]$, which is also called TKG completion. In contrast, the extrapolation setting aims to predict possible events after the given time t_n , i.e., inferring the entity o (or s) given query $q = (s, p, ?, t)$ (or $(?, p, o, t)$) where $t > t_n$.

Models in the former case such as HyTE [23], TeMP [24], and ChronoR [25] are designed to infer missing relations within the observed data. However, such models are not designed to predict future events that fall out of the specified time interval. In the latter case, various methods are designed for the purpose of future event prediction. Know-Evolve [26] is the first model to learn non-linearly evolving entity embeddings, yet unable to capture the long-term dependency due to the lack of investigation on historical events. xERTE [27] and TLogic [17] provide understandable evidence that can explain the forecast, but their application scenarios are limited. TANGO [18] employs neural ordinary differential equations to model the TKGs. A copy-generation mechanism is adopted in CyGNet [28] to identify high-frequency repetitive events. CluSTeR [16] is designed with reinforcement learning, yet constraining its applicability to event-based TKGs. There also emerge some models which try to adopt GNN [29] or RNN architecture to capture spatial temporal patterns. For instance, RE-NET [13] formulates the temporal link prediction in an autoregressive fashion, which utilizes RGCN [30] and GRU to capture the spatio-temporal dependencies. RE-GCN [14] and TiRGN [20] learn the evolutionary representations of entities and relations with Graph Convolution Network (GCN) [29] at each timestamp by modeling the KG sequence recurrently. HIP [19] models the temporal evolution of events, the interactions of concurrent events, and the known events respectively. EvoKG [21] captures the ever-changing structural and temporal dynamics in TKGs via recurrent event modeling based on the temporal neighborhood aggregation framework.

TABLE 1
The use of historical information in different methods.

Method	Technique	Historical Information
RE-NET	RNN	Time-window (10)
xERTE	Time-Vector	ALL with weighted sample
CluSTeR	LSTM+GRU	Time-window (<10)
Tlogic	Time-Operation	Time-window (> 30)
RE-GCN	GRU	Time-window (<10)
TANGO	Neural Ordinary Equations	Time-window (<10)
CyGNet	Time-Vector	ALL
TiRGN	GRU	Time-window (<15)
EvoKG	RNN	Time-window (<40)
HIP	GRU	Time-window (<20)

The effective mining of historical information plays a crucial role for knowledge graph extrapolation. The historical information here refers to the query-specific events, repeatability, periodicity, etc. Table 1 shows the use of historical information in different methods. Most methods only consider part of the historical information, that is, use the time-window to select and truncate the latest timestamps, which will actually lead to the loss of information [17]. Therefore, in our scenario, we tend to explore the occurrence pattern of events from all data.

2.2 Contrastive Learning

Contrastive learning as a self-supervised learning paradigm focuses on distinguishing instances of different categories. In self-supervised contrastive learning, most methods [31] derive augmented examples from a randomly sampled minibatch of N examples, resulting in $2N$ samples to optimize the following loss function given a positive pair of examples (i, j) . Equation 1 is the contrastive loss:

$$\mathcal{L}_{i,j} = -\log \frac{\exp(\mathbf{z}_i \cdot \mathbf{z}_j / \tau)}{\sum_{k=1, k \neq i}^{2N} \exp(\mathbf{z}_i \cdot \mathbf{z}_k / \tau)}, \quad (1)$$

where \mathbf{z}_i is the projection embedding of sample i and $\tau \in \mathbb{R}^+$ denotes a temperature parameter helping the model learn from hard negatives. According to the contrastive predictive coding [32], minimizing the loss $\mathcal{L}_{i,j}$ leads to maximizing a lower-bound of mutual information between i and j . In the case of supervised learning, there is a work [33] generalizing contrastive loss to an arbitrary number of positives, which separates the representations of different instances using ground truth labels. The obtained contrastive representations can promote the downstream classifier to achieve better performance compared with vanilla classification model. TKG reasoning is a supervised task where we design a historical contrastive learning strategy to predict future events.

3 METHOD

As shown in Figure 4, CENET captures both the historical and non-historical dependency. Simultaneously, it utilizes contrastive learning to identify highly correlated entities. A mask-based inference process is further employed for reasoning performing. In the following parts, we will introduce our proposed method in detail.

3.1 Preliminaries

Let \mathcal{E} , \mathcal{R} , and \mathcal{T} denote a finite set of entities, relation types, and timestamps, respectively. A temporal knowledge graph \mathcal{G} is a set of quadruples formalized as (s, p, o, t) , where $s \in \mathcal{E}$ is a subject (head) entity, $o \in \mathcal{E}$ is an object (tail) entity, $p \in \mathcal{R}$ is the relation (predicate) occurring at timestamp t between s and o . \mathcal{G}_t represents a TKG snapshot which is the set of quadruples occurring at time t . We use boldfaced \mathbf{s} , \mathbf{p} , \mathbf{o} for the embedding vectors of s , p , and o respectively, the dimension of which is d . $\mathbf{E} \in \mathbb{R}^{|\mathcal{E}| \times d}$ is the embeddings of all entities, the row of which represents the embedding vector of an entity such as \mathbf{s} and \mathbf{o} . Similarly, $\mathbf{P} \in \mathbb{R}^{|\mathcal{R}| \times d}$ is the embeddings of all relation types.

Given a query $q = (s, p, ?, t)$, we define the set of *historical events* as $\mathcal{D}_t^{s,p}$ and the corresponding set of *historical entities* as $\mathcal{H}_t^{s,p}$ in the following equations:

$$\mathcal{D}_t^{s,p} = \bigcup_{k < t} \{(s, p, o, k) \in \mathcal{G}_k\}, \quad (2)$$

$$\mathcal{H}_t^{s,p} = \{o | (s, p, o, k) \in \mathcal{D}_t^{s,p}\}. \quad (3)$$

Naturally, entities not in $\mathcal{H}_t^{s,p}$ are called *non-historical entities*, and the set $\{(s, p, o', k) | o' \notin \mathcal{H}_t^{s,p}, k < t\}$ denotes the set of *non-historical events*, where some quadruples may not exist in \mathcal{G} . It is worth noting that we also use $\mathcal{D}_t^{s,p}$ to represent

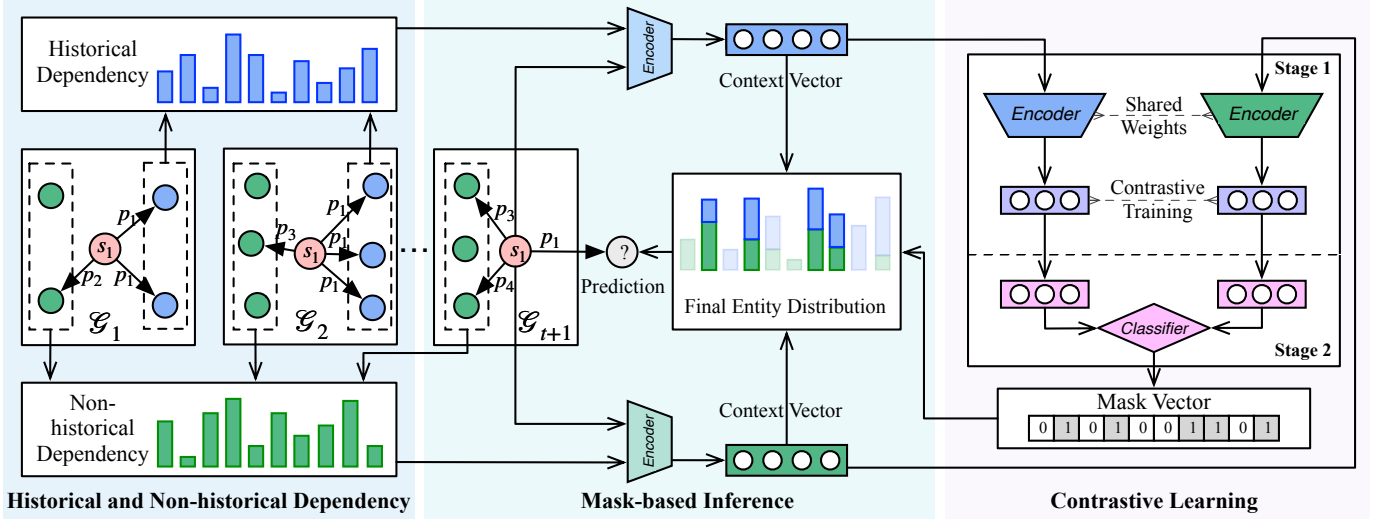


Fig. 4. The overall architecture of GENET. The left part learns the distribution of entities from both historical and non-historical dependency. The right part illustrates the two stages of historical contrastive learning, which aims to identify highly correlated entities, and the output is a boolean mask vector. The middle part is the mask-based inference process that combines the distribution learned from the two kinds of dependency and the mask vector to generate the final results.

the set of historical events for a current event (s, p, o, t) . If an event (s, p, o, t) itself does not exist in its corresponding $\mathcal{D}_t^{s,p}$, then it is a new event. Without loss of generality, we detail how CENET predicts object entities with a given query $q = (s, p, ?, t)$ in the following parts.

3.2 Historical and Non-historical Dependency

In most TKGs, although many events often show repeated occurrence pattern, new events may have no historical events to refer to. To this end, CENET takes not only historical but also non-historical entities into consideration. During data pre-processing, we first investigate the frequencies of historical entities for the given query $q = (s, p, ?, t)$ in the entire timeline without truncation operation. More specifically, we count the frequencies $\mathbf{F}_t^{s,p} \in \mathbb{R}^{|\mathcal{E}|}$ of all entities served as the objects associated with subject s and predicate p before time t , as shown in Equation 4:

$$\mathbf{F}_t^{s,p}(o) = \sum_{k < t} |\{o | (s, p, o, k) \in \mathcal{G}_k\}|. \quad (4)$$

Since we cannot count the frequencies of non-historical entities, CENET transforms $\mathbf{F}_t^{s,p}$ into $\mathbf{Z}_t^{s,p} \in \mathbb{R}^{|\mathcal{E}|}$ where the value of each slot is limited by a hyper-parameter λ :

$$\mathbf{Z}_t^{s,p}(o) = \lambda \cdot (\Phi_{\mathbf{F}_t^{s,p}(o) > 0} - \Phi_{\mathbf{F}_t^{s,p}(o) = 0}). \quad (5)$$

Φ_β is an indicator function that returns 1 if β is true and 0 otherwise. $\mathbf{Z}_t^{s,p}(o) > 0$ represents the quadruple (s, p, o, t_k) is a historical event bound to s, p , and t ($t_k < t$), while $\mathbf{Z}_t^{s,p}(o) < 0$ indicates that the quadruple (s, p, o, t_k) is a non-historical event that does not exist in \mathcal{G} . Next, CENET learns the dependency from both the historical and non-historical events based on the input $\mathbf{Z}_t^{s,p}$. CENET adopts a copy mechanism based learning strategy [34] to capture different kinds of dependency from two aspects: one is the similarity score vector between query and the set of entities, the other is the query's corresponding frequency information with copy mechanism.

For historical dependency, CENET generates a latent context vector $\mathbf{H}_{his}^{s,p} \in \mathbb{R}^{|\mathcal{E}|}$ for query q , which scores the historical dependency of different object entities:

$$\mathbf{H}_{his}^{s,p} = \underbrace{\tanh(\mathbf{W}_{his}(\mathbf{s} \oplus \mathbf{p}) + \mathbf{b}_{his})\mathbf{E}^T}_{\text{similarity score between } q \text{ and } \mathcal{E}} + \mathbf{Z}_t^{s,p}, \quad (6)$$

where \tanh is the activation function, \oplus represents the concatenation operator, $\mathbf{W}_{his} \in \mathbb{R}^{d \times 2d}$ and $\mathbf{b}_{his} \in \mathbb{R}^d$ are trainable parameters. We use a linear layer with \tanh activation to aggregate the query's information. The output of the linear layer is then multiplied by \mathbf{E} to obtain an $|\mathcal{E}|$ -dimensional vector, where each element represents the **similarity** score between the corresponding entity $o' \in \mathcal{E}$ and the query q . Then, according to the copy mechanism, we add the copy-term $\mathbf{Z}_t^{s,p}$ to change the index scores of historical entities in $\mathbf{H}_{his}^{s,p}$ to higher values directly without contributing to the gradient update. Thus, $\mathbf{Z}_t^{s,p}$ makes $\mathbf{H}_{his}^{s,p}$ pay more attention to historical entities. Similarly, for non-historical dependency, the latent context vector $\mathbf{H}_{nhis}^{s,p}$ is defined as:

$$\mathbf{H}_{nhis}^{s,p} = \tanh(\mathbf{W}_{nhis}(\mathbf{s} \oplus \mathbf{p}) + \mathbf{b}_{nhis})\mathbf{E}^T - \mathbf{Z}_t^{s,p}. \quad (7)$$

Contrary to historical dependency (Equation 6), subtracting $\mathbf{Z}_t^{s,p}$ makes $\mathbf{H}_{nhis}^{s,p}$ focus on non-historical entities. The training objective of learning from both historical and non-historical events is to minimize the following loss \mathcal{L}^{ce} :

$$\mathcal{L}^{ce} = - \sum_q \log \left\{ \frac{\exp(\mathbf{H}_{his}^{s,p}(o_i))}{\sum_{o_j \in \mathcal{E}} \exp(\mathbf{H}_{his}^{s,p}(o_j))} + \frac{\exp(\mathbf{H}_{nhis}^{s,p}(o_i))}{\sum_{o_j \in \mathcal{E}} \exp(\mathbf{H}_{nhis}^{s,p}(o_j))} \right\}, \quad (8)$$

where o_i denotes the ground truth object entity of the given query q . The purpose of \mathcal{L}^{ce} is to separate ground truth from others by comparing each scalar value in $\mathbf{H}_{his}^{s,p}$ and $\mathbf{H}_{nhis}^{s,p}$.

During the inference, CENET combines the softmax results of the above two latent context vectors as the predicted probabilities $\mathbf{P}_t^{s,p}$ over all object entities:

$$\mathbf{P}_t^{s,p} = \frac{1}{2} \{ \text{softmax}(\mathbf{H}_{his}^{s,p}) + \text{softmax}(\mathbf{H}_{nhis}^{s,p}) \}, \quad (9)$$

where the entity with maximum value is the most likely entity the component predicts. To be noted, capturing historical and non-historical dependency is an indispensable part of CENET, and $\mathbf{P}_t^{s,p}$ is the basis of historical contrastive learning during the inference.

3.3 Historical Contrastive Learning

Clearly, the learning mechanism defined above well captures the historical and non-historical dependency for each query. However, many repetitive and periodic events are only associated with historical entities. Besides, for new events, existing models are likely to ignore those entities with less historical interaction and predict the wrong entities that frequently interact with other events. The proposed historical contrastive learning trains contrastive representations of queries to identify a small number of highly correlated entities at the query level.

Specifically, the training process of supervised contrastive learning [33] consists of two stages. We first introduce I_q to indicate whether the missing object is in $\mathcal{H}_t^{s,p}$ for query q . In other words, if I_q is equal to 1, the missing object of the given query q is in $\mathcal{H}_t^{s,p}$, and 0 otherwise. The aim of the two stages is to train a binary classifier which infers the value of such boolean scalar for query q . Figure 5 illustrates the training process of historical contrastive learning.

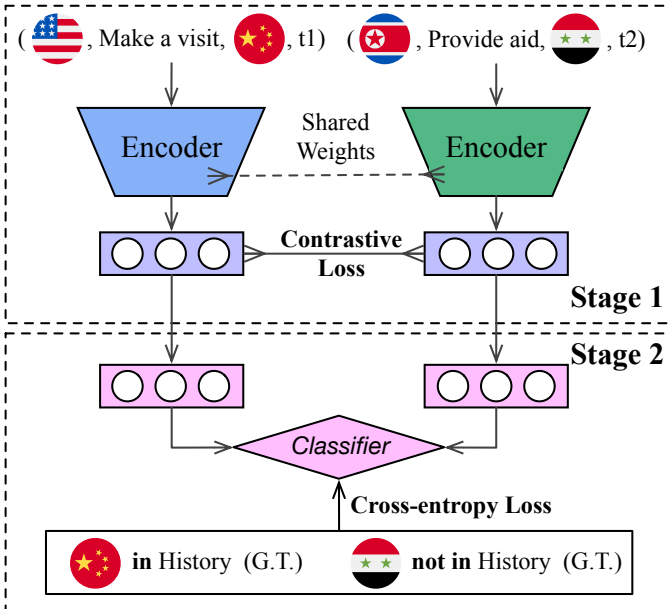


Fig. 5. The detail of historical contrastive learning: CENET learns representations using a contrastive loss in stage 1, then trains a binary classifier using cross-entropy loss in stage 2.

Stage 1: Learning Contrastive Representations. In the first stage, the model learns the contrastive representations of queries by minimizing supervised contrastive loss, which takes whether I_q is positive as the training criterion to

separate representations of different queries as far as possible in semantic space. Let \mathbf{v}_q be the embedding vector (representation) of the given query q :

$$\mathbf{v}_q = MLP(\mathbf{s} \oplus \mathbf{p} \oplus \tanh(\mathbf{W}_F \mathbf{F}_t^{s,p})), \quad (10)$$

where the query's information is encoded by an MLP to normalize and project the embedding onto the unit sphere for further contrastive training. Let M denote the minibatch, $Q(q)$ denote the set of queries in the M except q whose boolean labels are the same as I_q , given as:

$$Q(q) = \bigcup_{m \in M \setminus \{q\}} \{m | I_m = I_q\}. \quad (11)$$

The detail of computing supervised contrastive loss \mathcal{L}^{sup} in the first stage is as follows:

$$\mathcal{L}^{sup} = \sum_{q \in M} \frac{-1}{|Q(q)|} \sum_{k \in Q(q)} \log \frac{\exp(\mathbf{v}_q \cdot \mathbf{v}_k / \tau)}{\sum_{a \in M \setminus \{q\}} (\mathbf{v}_q \cdot \mathbf{v}_a / \tau)}, \quad (12)$$

where, $\mathbf{W}_F \in \mathbb{R}^{d \times |\mathcal{E}|}$ is the trainable parameter, $\tau \in \mathbb{R}^+$ is the temperature parameter set to 0.1 in experiments as recommended in the previous work [33]. The objective of \mathcal{L}^{sup} is to make the representations of the same category closer. It should be noted that the contrastive supervised loss \mathcal{L}^{sup} and the previous cross-entropy-like loss \mathcal{L}^{ce} are trained simultaneously.

Stage 2: Training Binary Classifier. When the training of the first stage is finished, CENET freezes the weights of corresponding parameters including \mathbf{E} , \mathbf{P} and their encoders in the first stage. Then it feeds \mathbf{v}_q to a linear layer to train a binary classifier with cross-entropy loss according to the ground truth I_q , which is trivial to mention. Now, the classifier can recognize whether the missing object entity of query q exists in the set of historical entities. Removing stage 1 will degrade the performance of the binary classifier, in which case all queries are not well separated in semantic space.

In the process of reasoning, a boolean mask vector $\mathbf{B}_t^{s,p} \in \mathbb{R}^{|\mathcal{E}|}$ is generated to identify which kind of entities should be concerned according to the predicted \hat{I}_q and whether $o \in \mathcal{H}_t^{s,p}$ is true:

$$\mathbf{B}_t^{s,p}(o) = \Phi_{o \in \mathcal{H}_t^{s,p} = \hat{I}_q}. \quad (13)$$

The probabilities of entities in all positive positions ($\mathbf{B}_t^{s,p}(o) = 1$) will be further increased, and vice versa. In other words, if the missing object is predicted to be in $\mathcal{H}_t^{s,p}$, then entities in the historical set will receive more attention. Otherwise, those entities outside the historical set are more likely to be attended.

3.4 Parameter Learning and Inference

We minimize the loss function in the first stage:

$$\mathcal{L} = \alpha \cdot \mathcal{L}^{ce} + (1 - \alpha) \cdot \mathcal{L}^{sup}, \quad (14)$$

where α is a hyper-parameter ranging from 0 to 1 to balance different losses. Minimizing \mathcal{L}^{ce} enables the model to learn from historical and non-historical events. Minimizing the supervised contrastive loss \mathcal{L}^{sup} not only learns a good

Algorithm 1 Learning algorithm of CENET

Input: Observed graph quadruples set \mathcal{G} , entity set \mathcal{E} , relation type set \mathcal{R} , hyper-parameter α , and λ .

Output: A trained network.

- 1: Initiate parameters of network Net ;
 - 2: **for** each (s, p, o, t) in \mathcal{G} **do**
 - 3: Compute $\mathcal{H}_t^{s,p}$, $\mathbf{F}_t^{s,p}$, and $\mathbf{Z}_t^{s,p}$ for query $(s, p, ?, t)$ according to Eq.3, 4, and 5 respectively;
 - 4: Label I_q for query $(s, p, ?, t)$ using $\mathcal{H}_t^{s,p}$;
 - 5: **end for**
 - 6: **while** loss does not converge **do**
 - 7: Compute $\mathbf{H}_{his}^{s,p}$ and $\mathbf{H}_{nhis}^{s,p}$ using $\mathbf{Z}_t^{s,p}$ according to Eq.6 and 7 for each (s, p, o, t) in \mathcal{G} ;
 - 8: Compute \mathbf{v}_q using $\mathbf{F}_t^{s,p}$ according to Eq.10;
 - 9: Compute \mathcal{L}^{ce} using $\mathbf{H}_{his}^{s,p}$ and $\mathbf{H}_{nhis}^{s,p}$ according to Eq.8;
 - 10: Compute \mathcal{L}^{sup} using \mathbf{v}_q according to Eq.12;
 - 11: $\mathcal{L} \leftarrow \alpha \cdot \mathcal{L}^{ce} + (1 - \alpha) \cdot \mathcal{L}^{sup}$;
 - 12: Optimize Net according to \mathcal{L} ;
 - 13: **end while**
 - 14: Freeze parameters of Net except the classification layer in the second stage;
 - 15: Train the classification layer in Net according to I_q and \mathbf{v}_q with binary cross-entropy;
 - 16: **return** Net ;
-

representation of queries to identify their preference of object entities but also indirectly helps CENET capture historical and non-historical dependency via optimizing the embeddings of entities and relations in different queries. As to the second stage, we choose binary cross-entropy with sigmoid activation to train the binary classifier. Taking the prediction of object entities as an example, the detailed training process of CENET is provided in Algorithm 1. Such a training process is also used to predict the missing subject entities in the experiments.

As can be seen from Figure 4, the middle part illustrates the inference process that receives the distribution $\mathbf{P}_t^{s,p}$ and the mask vector $\mathbf{B}_t^{s,p}$ from both sides respectively. Then, CENET will choose the object with the highest probability as the final prediction \hat{o} :

$$\mathbf{P}(o|s, p, \mathbf{F}_t^{s,p}) = \mathbf{P}_t^{s,p}(o) \cdot \mathbf{B}_t^{s,p}(o), \quad (15)$$

$$\hat{o} = \operatorname{argmax}_{o \in \mathcal{E}} \mathbf{P}(o|s, p, \mathbf{F}_t^{s,p}). \quad (16)$$

Additionally, it is possible that a poor classifier of the second stage of historical contrastive learning may deteriorate the performance when wrongly masking the expected object entities. Thus, there is a compromised substitution:

$$\mathbf{P}(o|s, p, \mathbf{F}_t^{s,p}) = \mathbf{P}_t^{s,p}(o) \cdot \operatorname{softmax}(\mathbf{B}_t^{s,p})(o). \quad (17)$$

We call the former version in Equation 15 *hard-mask*, the latter in Equation 17 *soft-mask*. The hard-mask can reduce the search space and the soft-mask can obtain a more convincing distribution which makes the model more conservative.

3.5 Complexity Analysis

We analyze the complexity of the whole framework of historical contrastive learning in the stage of training and inference. For a minibatch M , the time complexity of learning the historical and non-historical dependency is $O(|M||\mathcal{E}|)$. Training the contrastive representation has the time complexity of $O(|M|^2)$ to calculate the similarity matrix for supervised contrastive loss. Thus, the computational complexity of training is $O(|M||\mathcal{E}| + |M|^2)$, and the inference complexity for a single query is $O(|\mathcal{E}|)$ since we only need to calculate the final distribution. The total space complexity is $O(|\mathcal{R}| + |\mathcal{E}| + L)$, where L is the number of layers of neural modules.

4 EXPERIMENTS

This section conducts a series of experiments to validate the performance of CENET. We first present the experimental settings and then compare CENET with a wide selection of TKG models. After that, the ablation study is implemented to evaluate the effectiveness of various components. Finally, the analysis of hyper-parameter is discussed. All our datasets and codes are publicly available¹.

4.1 Experimental Settings

4.1.1 Datasets

We select five benchmark datasets, including three event-based TKGs and two public KGs. These two types of datasets are constructed in different ways. The former three event-based TKGs consist of *Integrated Crisis Early Warning System* (ICEWS18 [15] and ICEWS14 [26]) and *Global Database of Events, Language, and Tone* (GDEL [35]) where a single event may happen at any time. The last two public KGs (WIKI [36] and YAGO [37]) consist of temporally associated facts which last a long time and hardly occur in the future. Table 2 provides the statistics of these datasets.

As mentioned earlier, the number of new events has a great impact on the performance of different models. We provide the rates of new events on different training datasets. It can be observed that there are a large proportion of new events in event-based TKGs (ICEWS18, ICEWS14, and GDEL). In terms of all public KGs (WIKI and YAGO), the rates of new events are lower than 20%. Predicting new events is a challenge for many autoregressive models because mining the non-historical dependency is difficult. Our proposed historical contrastive learning addresses the issue to some extent. For the datasets with lower rates of new events, fewer new events are beneficial to the training of the binary classifier in the Oracle, where the numbers of different I_q values are imbalanced.

4.1.2 Baselines

CENET is compared with 22 up-to-date knowledge graph reasoning models, including static and temporal approaches. Static methods include TransE [38], DistMult [39], ComplEx [40], R-GCN [30], ConvE [41], and RotatE [42]. Temporal models include HyTE [23], TTransE [43], TA-DistMult [12], DySAT [44], TeMP [24], DyRep+MLP [45],

1. <https://github.com/xyjigsaw/CENET>

TABLE 2
Statistics of the datasets.

Dataset	Entities	Relation	Training	Validation	Test	Granularity	Time Granules	Proportion of New Events
ICEWS18	23,033	256	373,018	45,995	49,545	24 hours	304	58.86% (Training)
ICEWS14	12,498	260	323,895	-	341,409	24 hours	365	53.85% (Training)
GDELTA	7,691	240	1,734,399	238,765	305,241	15 mins	2,751	44.97% (Training)
WIKI	12,554	24	539,286	67,538	63,110	1 year	232	2.8% (Training)
YAGO	10,623	10	161,540	19,523	20,026	1 year	189	10.4% (Training)

TABLE 3

Experimental results of temporal link prediction on three event-based TKGs. $\gg 1$ day means running time is more than 1 day. The best results are boldfaced, and the results of previous SOTAs are underlined.

Method	ICEWS18				ICEWS14				GDELTA			
	MRR	Hits@1	Hits@3	Hits@10	MRR	Hits@1	Hits@3	Hits@10	MRR	Hits@1	Hits@3	Hits@10
TransE	17.56	2.48	26.95	43.87	18.65	1.12	31.34	47.07	16.05	0.00	26.10	42.29
DistMult	22.16	12.13	26.00	42.18	19.06	10.09	22.00	36.41	18.71	11.59	20.05	32.55
CompLex	30.09	21.88	34.15	45.96	24.47	16.13	27.49	41.09	22.77	15.77	24.05	36.33
R-GCN	23.19	16.36	25.34	36.48	26.31	18.23	30.43	45.34	23.31	17.24	24.96	34.36
ConvE	36.67	28.51	39.80	50.69	40.73	33.20	43.92	54.35	35.99	27.05	39.32	49.44
RotatE	23.10	14.33	27.61	38.72	29.56	22.14	32.92	42.68	22.33	16.68	23.89	32.29
HyTE	7.31	3.10	7.50	14.95	11.48	5.64	13.04	22.51	6.37	0.00	6.72	18.63
TTransE	8.36	1.94	8.71	21.93	6.35	1.23	5.80	16.65	5.52	0.47	5.01	15.27
TA-DistMult	28.53	20.30	31.57	44.96	20.78	13.43	22.80	35.26	29.35	22.11	31.56	41.39
DySAT	19.95	14.42	23.67	26.67	18.74	12.23	19.65	21.17	23.34	14.96	22.57	27.83
TeMP	40.48	33.97	42.63	52.38	43.13	35.67	45.79	56.12	37.56	29.82	40.15	48.60
DyRep+MLP	9.86	5.14	10.66	18.66	24.61	15.88	28.87	39.34	23.94	15.57	27.88	36.58
R-GCRN+MLP	35.12	27.19	38.26	50.49	36.77	28.63	40.15	52.33	37.29	29.00	41.08	51.88
RE-NET	42.93	36.19	45.47	55.80	45.71	38.42	49.06	59.12	40.12	32.43	43.40	53.80
xERTE	36.95	30.71	40.38	49.76	32.92	26.44	36.58	46.05		$\gg 1$ day		
TLogic	37.52	30.09	40.87	52.27	38.19	32.23	41.05	49.58	22.73	17.65	24.66	32.59
RE-GCN	32.78	24.99	35.54	48.01	32.37	24.43	35.05	48.12	29.46	21.74	32.01	43.62
TANGO-Tucker	44.56	37.87	47.46	57.06	46.42	38.94	50.25	59.80	38.00	28.02	43.91	53.70
TANGO-Distmult	44.00	38.64	45.78	54.27	46.68	41.20	48.64	57.05	41.16	35.11	43.02	52.58
CyGNet	46.69	40.58	49.82	57.14	48.63	41.77	52.50	60.29	50.29	44.53	54.69	60.99
EvoKG	29.67	12.92	33.08	58.32	18.30	6.30	19.43	39.37	11.29	2.93	10.84	25.44
HIP	<u>48.37</u>	<u>43.51</u>	<u>51.32</u>	<u>58.49</u>	<u>50.57</u>	<u>45.73</u>	<u>54.28</u>	<u>61.65</u>	<u>52.76</u>	<u>46.35</u>	<u>55.31</u>	<u>61.87</u>
CENET	51.06	47.10	51.92	58.82	53.35	49.61	54.07	60.62	58.48	55.99	58.63	62.96

R-GCRN+MLP [46], RE-NET [13], xERTE [27], TLogic [17], RE-GCN [14], TANGO-Tucker [18], TANGO-Distmult [18], CyGNet [28], EvoKG [21], and HIP [19]. Some of the temporal baselines (HyTE, TTransE, and TeMP) are not applicable to event forecasting since they are proposed to handle graph interpolation, whereas our work focuses on the extrapolation task. Thus, we deal with them in the way of previous work [13], [19], [28], which is trivial to mention.

4.1.3 Training Settings and Evaluation Metrics

All datasets except ICEWS14 are split into training set (80%), validation set (10%), and testing set (10%). The original ICEWS14 is not provided with a validation set. We report a widely used filtered version [13], [19], [27], [28] of Mean Reciprocal Ranks (MRR) and Hits@1/3/10 (the proportion of correct predictions ranked within top 1/3/10). As to model configurations, we set the batch size to 1024, embedding dimension to 200, learning rate to 0.001, and use Adam optimizer. The training epoch for \mathcal{L} is limited to 30, and the epoch for the second stage of contrastive learning is limited to 20. The value of hyper-parameter α is set to 0.2, and λ is set to 2. For the settings of baselines, we use their

recommended configurations. All experiments are carried out on NVIDIA GeForce RTX 3090.

4.2 Results

4.2.1 Results on Event-based TKGs

Table 3 presents the MRR and Hits@1/3/10 results of link (event) prediction on three event-based TKGs. Our proposed CENET outperforms other baselines in most cases. It can be observed that many static models are inferior to temporal models because static models do not consider temporal information and their dependency between different snapshots. In the case of temporal models, TeMP is designed to complete missing links (graph interpolation) rather than predict new events, and it thus shows worse performance than extrapolation models. Although xERTE provides a certain degree of predictive explainability, it is computationally inefficient to handle large-scale datasets such as GDELTA, whose training set contains more than 1 million samples. In terms of Hits@10, CENET is on par with HIP on these three event-based datasets. Nevertheless, the results of Hits@1 improve the most in our model. CENET achieves up to **8.25%**, **8.48%**, and **20.80%** improvements

of Hits@1 on ICEWS18, ICEWS14, and GDELT respectively. The main reason is that there exist a large proportion of new events without historical events in event-based datasets. CENET learns the historical and non-historical dependency of new events simultaneously, which mines those unobserved underlying factors. In contrast, models including TANGO and HIP perform well in terms of Hits@10 but cannot predict the correct entities exactly, making Hits@1 much lower than ours.

TABLE 4
Experimental results of temporal link prediction on two public KGs.

Method	WIKI			YAGO		
	MRR	Hits@1	Hits@3	MRR	Hits@1	Hits@3
TransE	46.68	36.19	49.71	48.97	46.23	62.45
DistMult	46.12	37.24	49.81	59.47	52.97	60.91
ComplEx	47.84	38.15	50.08	61.29	54.88	62.28
R-GCN	37.57	28.15	39.66	41.30	32.56	44.44
ConvE	47.57	38.76	50.10	62.32	56.19	63.97
RotatE	50.67	40.88	50.71	65.09	57.13	65.67
HyTE	43.02	34.29	45.12	23.16	12.85	45.74
TTransE	31.74	22.57	36.25	32.57	27.94	43.39
TA-DistMult	48.09	38.71	49.51	61.72	52.98	65.32
DySAT	31.82	22.07	26.59	43.43	31.87	43.67
TeMP	49.61	46.96	50.24	62.25	55.39	64.63
DyRep+MLP	11.60	-	12.74	5.87	-	6.54
R-GCRN+MLP	47.71	-	48.14	53.89	-	56.06
RE-NET	51.97	48.01	52.07	65.16	63.29	65.63
xERTE		$\gg 1$ day		58.75	58.46	58.85
TLogic	57.73	57.43	57.88	1.29	0.49	0.85
RE-GCN	44.86	39.82	46.75	65.69	59.98	68.70
TANGO-Tucker	53.28	52.21	53.61	67.21	65.56	67.59
TANGO-Distmult	54.05	51.52	53.84	68.34	67.05	68.39
CyGNet	45.50	50.48	50.79	63.47	64.26	65.71
EvoKG	50.66	12.21	63.84	55.11	54.37	81.38
HIP	54.71	53.82	54.73	67.55	66.32	68.49
CENET	68.39	68.33	68.36	84.13	84.03	84.23

4.2.2 Results on Public KGs

CENET also outperforms the baselines in all metrics on WIKI and YAGO. As can be seen from Table 4, CENET significantly achieves the improvements up to **23.68% (MRR)**, **25.77% (Hits@1)**, and **7.08% (Hits@3)** over SOTA on public KGs. This is because the recurrence rates in these two datasets are imbalanced [28], and our model can easily handle such data. In terms of the WIKI dataset, 62.3% object entities associated with their corresponding facts (grouped by *(subject, relation)* tuples) have appeared repeatedly at least once in history. In contrast, the recurrence rate of subject entities (grouped by *(object, relation)* tuples) is 23.4%, which hinders many models learning from the historical information when inferring subject entities. CENET can effectively alleviate the problem of the imbalanced recurrence rate because the concurrent learning of historical and non-historical dependency can complement each other to generate the entity distribution. Also, the probability of selecting unrelated entities is greatly reduced on account of the binary classifier regardless of the imbalanced recurrence rate. Furthermore, we can see that the results of Hits@3 are close to Hits@10 on public KGs not only in CENET but also

in most methods. We believe the phenomenon is due to the distribution of public KGs, where temporally associated facts last a long time in these datasets, i.e., they exist in continuous several snapshots, leading to most models being capable of remembering these exact targets during training.

4.3 Ablation Study

We choose ICEWS18 and YAGO from event-based TKGs and public KGs respectively for ablation analysis. Next, we investigate the effectiveness of the historical/non-historical dependency, loss functions, and the mask-based inference. Table 5 shows the results of ablation, where CENET-soft-mask is our proposed model with the softmax operated mask vector in Equation 17.

4.3.1 Importance of historical and non-historical dependency.

CENET-his only considers the historical dependency while CENET-nhis keeps the non-historical dependency. Both of them employ the contrastive learning. The performance of CENET-his is better than CENET-nhis since most events can be traced to their historical events especially in event-based TKGs such as ICEWS18. Still, for CENET-nhis, it also works on event prediction to a certain extent. Thus, the results of these two variants indicate it is necessary to consider both dependencies at the same time.

4.3.2 Influence of contrastive learning.

We remove \mathcal{L}^{sup} and only retain \mathcal{L}^{ce} as the variant CENET- \mathcal{L}^{ce} . Note that the binary classifier is still trained without learning contrastive representations of queries. In the case of ICEWS18, the \mathcal{L}^{ce} is capable of achieving high results close to the proposed CENET, while the results in YAGO have **dropped about 7%** because removing \mathcal{L}^{sup} cannot separate the two classes of queries in semantic space as far as possible. Such results verify the positive influence of stage 1 in historical contrastive learning. Figure 6 illustrates the 2-d sphereized PCA projection of query embeddings, which are obtained after training CENET and CENET- \mathcal{L}^{ce} . The color represents the ground truth I_q , indicating whether the missing object is in $\mathcal{H}_t^{s,p}$. We can see there exists an explicit border between the two types of queries for CENET with \mathcal{L}^{sup} loss.

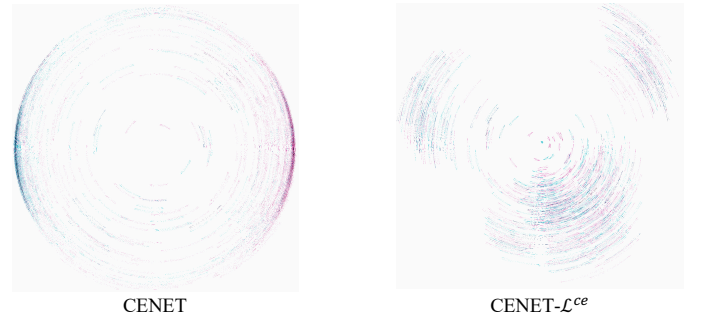


Fig. 6. Query embeddings with sphereized PCA projection on YAGO.

CENET-w/o-stage-2 is another variant that minimizes \mathcal{L}^{ce} and \mathcal{L}^{sup} without training the binary classifier, which naturally discards the mask-based inference. Such changes

TABLE 5
Ablation study of CENET on ICEWS18 and YAGO.

Method	ICEWS18				YAGO			
	MRR	Hits@1	Hits@3	Hits@10	MRR	Hits@1	Hits@3	Hits@10
CENET-his	50.65	47.15	51.23	57.42	71.64	70.24	71.81	74.39
CENET-nhis	31.75	24.22	34.01	46.69	61.73	59.64	62.50	65.38
CENET- \mathcal{L}^{ce} (w/o-stage-1)	50.59	46.47	51.58	58.58	75.25	73.96	75.55	77.52
CENET-w/o-stage-2	50.32	46.30	51.29	58.16	77.53	76.12	78.04	79.84
CENET-w/o-CL	49.98	45.89	50.74	57.81	73.29	71.87	73.64	75.90
CENET-random-mask	26.80	24.42	27.47	31.60	39.07	38.31	39.28	40.41
CENET-hard-mask	49.66	46.69	50.78	55.75	84.13	84.03	84.23	84.24
CENET-soft-mask	51.06	47.10	51.92	58.82	80.03	79.09	80.30	81.57
CENET-GT-mask	52.75	48.21	53.97	61.84	84.73	84.31	84.76	85.34

cause **1.7% and 3.8% drop** in terms of Hits@1 on ICEWS18 and YAGO respectively. CENET-w/o-CL removing the historical contrastive learning has worse performance than the above two variants. These results prove the significance of our proposed historical contrastive learning. Additionally, we can see that minimizing \mathcal{L}^{ce} can effectively handle event-based datasets, and \mathcal{L}^{sup} can further improve the performance of the model based on \mathcal{L}^{ce} in terms of public KGs. These results can be interpreted by the different properties and distributions of these two kinds of datasets. Specifically, for event-based TKGs, facts may happen multiple times, under which the circumstance is suitable for CENET to capture the historical and non-historical dependency. Facts in public KGs last a long time and hardly occur in the future whose representations are easy to be separated by \mathcal{L}^{sup} .

4.3.3 Influence of different variants of mask-based inference.

We also study different variants of mask strategy in CENET. The mask vector is a randomly generated boolean vector in CENET-random-mask. According to Equation 15 and 17, CENET-hard-mask and CENET-soft-mask are our proposed two ways to tackle the mask vector, and the latter is our used strategy. We use the ground truth in the testing set to generate a mask vector represented by CENET-GT-mask to explore the upper bound of CENET. As can be seen from Table 5, untrained model with randomly generated mask vector is counterproductive to the prediction. Moreover, CENET-soft-mask shows better results on ICEWS18 while CENET-hard-mask can handle YAGO more effectively. The results of CENET-hard-mask can even be close to the ground truth value for the reason that the accuracy of the binary classification in YAGO (about 90%) is higher than that in ICEWS18 (about 70%). Therefore, the higher the accuracy of the binary classification, the harder version of mask should be selected. In order to get the best trade-off on various TKG datasets, we use the soft-mask in our final model according to the results on the validation set.

4.4 Hyper-parameter Analysis

There are two unexplored hyper-parameters α and λ in CENET. We adjust the values of α and λ respectively to observe the performance change of CENET on ICEWS18 and YAGO. The results are shown in Figure 7. The hyper-parameter α aims at balancing the contribution of \mathcal{L}^{ce} and

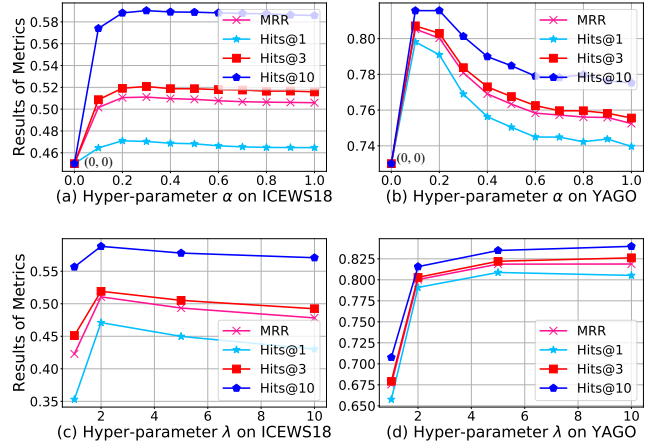


Fig. 7. Results of hyper-parameters α and λ of CENET on ICEWS18 and YAGO.

\mathcal{L}^{sup} . Due to the difference of characteristics between event-based TKGs and public KGs, the hyper-parameter α ranging from 0 to 1 leads to different results on these two kinds of datasets. Specifically, \mathcal{L}^{ce} contributes more to event-based TKGs, while \mathcal{L}^{sup} is more friendly to public KGs. Considering that if we remove \mathcal{L}^{ce} i.e. set α to 0, then we cannot obtain the final probability $\mathbf{P}(o|s, p, \mathbf{F}_t^{s,p})$ (and $\mathbf{P}(s|o, p, \mathbf{F}_t^{o,p})$) for inference. To this end, we set α to 0.2. With regard to the hyper-parameter λ , we first fix the value of hyper-parameter α , then the λ is analyzed. We can see that the higher the value of λ , the better the result on YAGO, whereas the worse the result on ICEWS18. Therefore, λ is set to 2.

4.5 Case Study

As shown in Figure 8, we select three representative queries with *North Korea* as subject entity to investigate the predicted results of CENET.

- Query (*North Korea*, *Halt negotiations*, *?*, *t*): It can be observed that the group (*Halt negotiations, the United States*) appears most frequently in the past (with blue font). It is easy for CENET to obtain the correct answer for the reason that the historical dependency has been captured, and the mask-based inference with a binary classifier can reduce the probabilities of non-historical entities such as *Russia and Singapore*

etc, which have nothing to do with the relation ‘*Halt negotiations*’.

- Query (*North Korea, Intent to cooperate, ?, t*): The group (*Intent to cooperate, South Korea*) only happened once (with red font), which is the same to other object entities such as *the United States and Russia*. Not surprisingly, the model can predict correctly. Although the *United States and North Korea* had the relation ‘*Intent to cooperate*’ in the past, CENET believes that other relations between the *United States and North Korea* were more likely to happen, the first case is the best evidence. Thus, the model chose *South Korea*.
- Query (*North Korea, Express accord, ?, t*): This query has no historical events from the first timestamp 0, but the model also gets the correct result, demonstrating that CENET has learned the non-historical dependency.

5 CONCLUSION AND FUTURE WORK

In this paper, we explore the limits of historical information in existing TKG methods and propose a novel temporal knowledge graph representation learning model, Contrastive Event Network (CENET), for event forecasting. The key idea of CENET is to learn a convincing distribution of the whole entity set and identify significant entities from both historical and non-historical dependency in the framework of contrastive learning. The experimental results present that CENET outperforms all existing methods in most metrics significantly, especially for Hits@1. Promising future work includes exploring the ability of contrastive learning in knowledge graph, such as finding more reasonable contrastive pairs. Besides, it is also meaningful to design an explainable reasoning model for predicting potential links on temporal knowledge graphs.

ACKNOWLEDGMENTS

This work was supported by NSF China (No. 62020106005, 42050105, 62061146002, 61960206002), 100-Talents Program of Xinhua News Agency, Shanghai Pilot Program for Basic Research - Shanghai Jiao Tong University, and the Program of Shanghai Academic/Technology Research Leader under Grant No. 18XD1401800.

REFERENCES

- [1] Y. Xu, J. Ou, H. Xu, and L. Fu, “Temporal knowledge graph reasoning with historical contrastive learning,” in *AAAI*, 2023.
- [2] T. Sun, Y. Shao, X. Qiu, Q. Guo, Y. Hu, X.-J. Huang, and Z. Zhang, “Colake: Contextualized language and knowledge embedding,” in *COLING*, 2020.
- [3] Q. Wang, M. Li, X. Wang, N. Parulian, G. Han, J. Ma, J. Tu, Y. Lin, H. Zhang, W. Liu *et al.*, “Covid-19 literature knowledge graph construction and drug repurposing report generation,” *arXiv preprint arXiv:2007.00576*, 2020.
- [4] L. Huang, L. Wu, and L. Wang, “Knowledge graph-augmented abstractive summarization with semantic-driven cloze reward,” in *Proceedings of the 58th Annual Meeting of the Association for Computational Linguistics*, 2020, pp. 5094–5107.
- [5] X. Wang, X. He, Y. Cao, M. Liu, and T.-S. Chua, “Kgat: Knowledge graph attention network for recommendation,” in *SIGKDD*, 2019.
- [6] Y. Yang, C. Huang, L. Xia, and C. Li, “Knowledge graph contrastive learning for recommendation,” in *Proceedings of the 45th International ACM SIGIR Conference on Research and Development in Information Retrieval*, ser. SIGIR ’22. Association for Computing Machinery, 2022, p. 1434–1443.
- [7] Z. Liu, C. Xiong, M. Sun, and Z. Liu, “Entity-duet neural ranking: Understanding the role of knowledge graph semantics in neural information retrieval,” in *ACL*, 2018.
- [8] Y. Zhou, X. Chen, B. He, Z. Ye, and L. Sun, “Re-thinking knowledge graph completion evaluation from an information retrieval perspective,” ser. SIGIR ’22. Association for Computing Machinery, 2022, p. 916–926.
- [9] S. Deng, H. Rangwala, and Y. Ning, “Dynamic knowledge graph based multi-event forecasting,” in *SIGKDD*, 2020.
- [10] F. Feng, X. He, X. Wang, C. Luo, Y. Liu, and T.-S. Chua, “Temporal relational ranking for stock prediction,” *TOIS*, vol. 37, no. 2, 2019.
- [11] Z. Jia, A. Abujabal, R. Saha Roy, J. Strötgen, and G. Weikum, “Tequila: Temporal question answering over knowledge bases,” in *CIKM*, 2018.
- [12] A. García-Durán and S. Dumančić, “Learning sequence encoders for temporal knowledge graph completion,” *arXiv preprint arXiv:1809.03202*, 2018.
- [13] W. Jin, M. Qu, X. Jin, and X. Ren, “Recurrent event network: Autoregressive structure inference over temporal knowledge graphs,” in *EMNLP*, 2020.
- [14] Z. Li, X. Jin, W. Li, S. Guan, J. Guo, H. Shen, Y. Wang, and X. Cheng, “Temporal knowledge graph reasoning based on evolutionary representation learning,” *arXiv preprint arXiv:2104.10353*, 2021.
- [15] E. Boschee, J. Lautenschlager, S. O’Brien, S. Shellman, J. Starz, and M. Ward, “Icews coded event data,” *Harvard Dataverse*, vol. 12, 2015.
- [16] Z. Li, X. Jin, S. Guan, W. Li, J. Guo, Y. Wang, and X. Cheng, “Search from history and reason for future: Two-stage reasoning on temporal knowledge graphs,” *arXiv preprint arXiv:2106.00327*, 2021.
- [17] Y. Liu, Y. Ma, M. Hildebrandt, M. Joblin, and V. Tresp, “Tlogic: Temporal logical rules for explainable link forecasting on temporal knowledge graphs,” *arXiv preprint arXiv:2112.08025*, 2021.
- [18] Z. Han, Z. Ding, Y. Ma, Y. Gu, and V. Tresp, “Learning neural ordinary equations for forecasting future links on temporal knowledge graphs,” in *EMNLP*, 2021, pp. 8352–8364.
- [19] Y. He, P. Zhang, L. Liu, Q. Liang, W. Zhang, and C. Zhang, “Hip network: Historical information passing network for extrapolation reasoning on temporal knowledge graph,” in *IJCAI*, 2021.
- [20] Y. Li, S. Sun, and J. Zhao, “Tirgn: Time-guided recurrent graph network with local-global historical patterns for temporal knowledge graph reasoning,” in *Proceedings of the Thirty-First International Joint Conference on Artificial Intelligence, IJCAI-22*, L. D. Raedt, Ed. International Joint Conferences on Artificial Intelligence Organization, 7 2022, pp. 2152–2158.
- [21] N. Park, F. Liu, P. Mehta, D. Cristoforo, C. Faloutsos, and Y. Dong, “Evokg: Jointly modeling event time and network structure for reasoning over temporal knowledge graphs,” in *WSDM*, 2022.
- [22] K. Liang, L. Meng, M. Liu, Y. Liu, W. Tu, S. Wang, S. Zhou, X. Liu, and F. Sun, “Reasoning over different types of knowledge graphs: Static, temporal and multi-modal,” *arXiv preprint arXiv:2212.05767*, 2022.
- [23] S. S. Dasgupta, S. N. Ray, and P. Talukdar, “Hyte: Hyperplane-based temporally aware knowledge graph embedding,” in *EMNLP*, 2018.
- [24] J. Wu, M. Cao, J. C. K. Cheung, and W. L. Hamilton, “Temp: Temporal message passing for temporal knowledge graph completion,” in *EMNLP*, 2020.
- [25] A. Sadeghian, M. Armandpour, A. Colas, and D. Z. Wang, “Chronor: Rotation based temporal knowledge graph embedding,” in *AAAI*, 2021.
- [26] R. Trivedi, H. Dai, Y. Wang, and L. Song, “Know-evolve: Deep temporal reasoning for dynamic knowledge graphs,” in *ICML*. PMLR, 2017.
- [27] Z. Han, P. Chen, Y. Ma, and V. Tresp, “Explainable subgraph reasoning for forecasting on temporal knowledge graphs,” in *ICLR*, 2020.
- [28] C. Zhu, M. Chen, C. Fan, G. Cheng, and Y. Zhang, “Learning from history: Modeling temporal knowledge graphs with sequential copy-generation networks,” in *AAAI*, vol. 35, 2021.





















History (p, o) with same s at different times			Query ($s, p, ?, t$)	Prediction	Answer
Halt negotiations 	Halt negotiations 	Halt negotiations 	s :  p : Halt negotiations		
Halt negotiations 	Intent to cooperate 	Intent to cooperate 	s :  p : Intent to cooperate		
Intent to cooperate 	Make a visit 	Make a visit 	s :  p : Express accord		
Make a visit 	Make a visit 	Make a visit			
$t - 3$	$t - 2$	$t - 1$	t		

Fig. 8. Case study of GENET’s predictions. We select three queries with North Korea as subject entity for analysis.

[29] T. N. Kipf and M. Welling, “Semi-supervised classification with graph convolutional networks,” *arXiv preprint arXiv:1609.02907*, 2016.

[30] M. Schlichtkrull, T. N. Kipf, P. Bloem, R. Van Den Berg, I. Titov, and M. Welling, “Modeling relational data with graph convolutional networks,” in *ESWC*. Springer, 2018.

[31] T. Chen, S. Kornblith, M. Norouzi, and G. Hinton, “A simple framework for contrastive learning of visual representations,” in *ICML*. PMLR, 2020.

[32] A. v. d. Oord, Y. Li, and O. Vinyals, “Representation learning with contrastive predictive coding,” *arXiv preprint arXiv:1807.03748*, 2018.

[33] P. Khosla, P. Teterwak, C. Wang, A. Sarna, Y. Tian, P. Isola, A. Maschinot, C. Liu, and D. Krishnan, “Supervised contrastive learning,” *arXiv preprint arXiv:2004.11362*, 2020.

[34] J. Gu, Z. Lu, H. Li, and V. O. Li, “Incorporating copying mechanism in sequence-to-sequence learning,” in *ACL*, 2016.

[35] K. Leetaru and P. A. Schrodt, “Gdelt: Global data on events, location, and tone, 1979–2012,” in *ISA annual convention*, vol. 2. Citeseer, 2013.

[36] J. Leblay and M. W. Chekol, “Deriving validity time in knowledge graph,” in *The Web Conference*, 2018.

[37] F. Mahdisoltani, J. Biega, and F. Suchanek, “Yago3: A knowledge base from multilingual wikipedias,” in *CIDR*. CIDR Conference, 2014.

[38] A. Bordes, N. Usunier, A. Garcia-Duran, J. Weston, and O. Yakhnenko, “Translating embeddings for modeling multi-relational data,” *NeurIPS*, vol. 26, 2013.

[39] B. Yang, W.-t. Yih, X. He, J. Gao, and L. Deng, “Embedding entities and relations for learning and inference in knowledge bases,” *arXiv preprint arXiv:1412.6575*, 2014.

[40] T. Trouillon, J. Welbl, S. Riedel, É. Gaussier, and G. Bouchard, “Complex embeddings for simple link prediction,” in *ICML*. PMLR, 2016.

[41] T. Dettmers, P. Minervini, P. Stenetorp, and S. Riedel, “Convolutional 2d knowledge graph embeddings,” in *AAAI*, 2018.

[42] Z. Sun, Z.-H. Deng, J.-Y. Nie, and J. Tang, “Rotate: Knowledge graph embedding by relational rotation in complex space,” *arXiv preprint arXiv:1902.10197*, 2019.

[43] T. Jiang, T. Liu, T. Ge, L. Sha, B. Chang, S. Li, and Z. Sui, “Towards time-aware knowledge graph completion,” in *COLING*, 2016.

[44] A. Sankar, Y. Wu, L. Gou, W. Zhang, and H. Yang, “Dysat: Deep neural representation learning on dynamic graphs via self-attention networks,” in *WSDM*, 2020.

[45] R. Trivedi, M. Farajtabar, P. Biswal, and H. Zha, “Dyrep: Learning representations over dynamic graphs,” in *ICLR*, 2019.

[46] Y. Seo, M. Defferrard, P. Vandergheynst, and X. Bresson, “Structured sequence modeling with graph convolutional recurrent networks,” in *NeurIPS*. Springer, 2018.



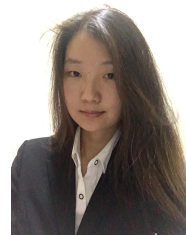
Yi Xu received the B.E. degree in Department of Computer Science and Technology from Anhui University, Hefei, China, in 2020. He is currently pursuing his Ph.D. degree in Department of Computer Science and Engineering from Shanghai Jiao Tong University. His research interests include data mining, knowledge graph and natural language processing.



Junjie Ou received the B.S. degree in information and communication engineering from Beijing Jiaotong University, Beijing, China, in 2018. He is currently pursuing the Ph.D. degree in information and communication engineering with Shanghai Jiao Tong University. His current research interests include data mining, information retrieval and recommendation system.



Hui Xu received his B.E. degree in School of Electronic and Information Engineering from Beijing Jiaotong University, China, in 2018. He is currently pursuing his Ph.D. degree in Department of Computer Science and Engineering in Shanghai Jiao Tong University. His research of interests are in the area of graph data mining, graph robust learning.



Luoyi Fu received her B.E. degree in Electronic Engineering from Shanghai Jiao Tong University, China, in 2009 and Ph.D. degree in Computer Science and Engineering in the same university in 2015. She is currently an Associate Professor in Department of Computer Science and Engineering in Shanghai Jiao Tong University. Her research of interests are in the area of social networking and big data, scaling laws analysis in wireless networks, connectivity analysis and random graphs. She has been a member of the Technical Program Committees of several conferences including ACM MobiHoc 2018-2023, IEEE INFOCOM 2018-2023.



Lei Zhou received his B.S. degree and M.S. degree from the Department of Oceanography, Ocean University of China, Qingdao, China. He received his Ph.D. degree in the Department of Atmospheric and Oceanic Sciences, University of Maryland, College Park, in 2009. Currently, he is a professor in the School of Oceanography, Shanghai Jiao Tong University, Shanghai, China. He is the editor of the Journal of Geophysical Research—Oceans and the chairman of the Physical Oceanography and Climate Committee of the North Pacific Marine Science Organization (PICES).



Xinbing Wang received the B.S. degree (with honors) from the Department of Automation, Shanghai Jiao Tong University, Shanghai, China, in 1998, and the M.S. degree from the Department of Computer Science and Technology, Tsinghua University, Beijing, China, in 2001. He received the Ph.D. degree, major in the Department of electrical and Computer Engineering, minor in the Department of Mathematics, North Carolina State University, Raleigh, in 2006. Currently, he is a professor in the Department of Electronic Engineering, Shanghai Jiao Tong University, Shanghai, China. Dr. Wang has been an associate editor for IEEE/ACM Transactions on Networking and IEEE Transactions on Mobile Computing, and the member of the Technical Program Committees of several conferences including ACM MobiCom 2012, 2018-2019, ACM MobiHoc 2012-2023, IEEE INFOCOM 2009-2023.



Chenghu Zhou received the B.S. degree from the Department of Geography, Nanjing University, China, in 1984, and the M.S. degree and Ph.D. degree from Institute of Geographical Sciences and Natural Resources Research, Chinese Academy of Sciences, China. He is an academican of Chinese Academy of Sciences and an academican of International Eurasian Academy of Sciences. Currently, he is the director of the State Key Laboratory of Resources and Environmental Information System. His research of interests are in the area of spatial data mining, geographic system modeling, hydrology and water resources, geographic information system and remote sensing application.